Hydro- and solvothermally-prepared ZnO and its catalytic effect on the photodegradation of Reactive Orange 16 dye

BOJANA SIMOVIĆ[1*#], ALEKSANDAR GOLUBOVIĆ[2#], IVANA VELJKOVIĆ[3], DEJAN POLETI[4#], JELENA ZDRAVKOVIĆ[5#], DUŠAN MIJIN[4#] and ANĐELIKA BJELAJAC[5#]

[1]*Institute for Multidisciplinary Research, University of Belgrade, Kneza Višeslava 1, 11030 Belgrade, Serbia,* [2]*Institute of Physics, University of Belgrade, Pregrevica 118, 11080 Belgrade-Zemun, Serbia,* [3]*The Netherlands Organization for Applied Scientific Research – TNO, De Rondom 1, Eindhoven, The Netherlands,* [4]*Department of General and Inorganic Chemistry, Faculty of Technology and Metallurgy, University of Belgrade, Karnegijeva 4, 11120 Belgrade, Serbia and* [5]*Innovation Centre – Faculty of Technology and Metallurgy, University of Belgrade, Karnegijeva 4, 11120 Belgrade, Serbia*

Abstract: In this work, zinc oxide powders were obtained by two different techniques: hydro- and solvothermal synthesis starting from $Zn(NO_3)_2$ and $Zn(CH_3COO)_2$, respectively. The influence of synthetic procedure on the structural, microstructural, thermal and photocatalytic properties of the prepared ZnO powders was investigated. Both ZnO samples were further annealed under moderate conditions (300 °C) to avoid grain growth and to remove traces of impurities. In all four cases, single-phase hexagonal ZnO was confirmed by X-ray powder diffraction. The morphologies of prepared ZnO powders were different and they varied from rounded nanograins to microrods. All prepared samples showed higher photocatalytic efficiency in the degradation of the textile azo dye Reactive Orange 16 (RO16) than commercial ZnO. In addition, the non-annealed samples had better photocatalytic properties than the commercial Degussa P25 TiO_2 powder.

Keywords: synthesis; ZnO powders; Reactive Orange 16; photocatalysis.

INTRODUCTION

Zinc oxide, ZnO, can be used in a large number of areas, since it is an inexpensive, chemically stable, easy to prepare and non-toxic material. ZnO has the ability to form a wide range of nanostructures: nanowires, nanorings, nanohoneycombs, nanorods, nanofibers, nanospheres, *etc*. Such ZnO nanopowders have

---

1433

initiated numerous studies,[1,2] and one of the many potential ZnO applications is in the ecological field.

Today most of water resources are polluted, and the contamination is constantly increasing due to rapid population growth, industrialization and urbanization. The wastewaters of the textile industries are the most polluting of all industrial sectors. Advanced oxidation processes are of interest for the effective oxidation of diverse organics and dyes. Among them, heterogeneous photocatalysis has become an important technology for the total mineralization of various organic pollutants, including reactive organic dyes.[3]

Most of the photocatalytic studies applied synthetic or commercial TiO_2 as the catalyst. However, the well-known employment of TiO_2 is not economic for large-scale water treatment and therefore attention has been drawn to the search for appropriate alternatives. Between many other semiconductors, ZnO appears to be a highly promising photocatalyst because it is one of the most important wide-band-gap materials with a direct band gap energy of 3.3 eV at room temperature, which corresponds to emission in the UV region.[1] In the last decades, the preparation fine ZnO nanopowders has attracted great interest. The great advantage of ZnO is that it absorbs a larger part of the solar spectrum than TiO_2. For this reason, ZnO is very suitable for photocatalytic degradation in the presence of both UV[4] and visible light.[5] For example, the photodegradation of Acid Brown 14 was studied by Sakthivel *et al*.[5] using ZnO irradiated with solar light. It is found that the photodegradation efficiency decreased with increasing initial dye concentration and optimum catalyst loading was 250 mg in 100 mL. Akyol *et al*.[6] studied the photocatalytic decolorization of Remazol Red by ZnO under UV light. Pandurangan *et al*.[7] realized the photodegradation of Basic Yellow Auramine O using ZnO exposed to solar radiation.

Studies that compared the efficiency of different catalysts for a particular dye under identical conditions are scarce.[5,6,8,9] For example, Daneshvar *et al*.[8] reported that ZnO is a suitable alternative to TiO_2 for the degradation of Acid red 14 azo dye. It was also found that the photodegradation mechanism of the dye by ZnO was similar to that by TiO_2.[8,9]

To the best of our knowledge, there are only three studies in which the photodegradation of RO16 dye by ZnO was attempted. In the first case, a ZnO suspension,[10] in the second one ZnO plates,[11] and in the third one ZnO coated thin film[12] were used. However, although many details were clarified, in all cases commercial ZnO was used as a catalyst, but only once[11] was it ball milled before the preparation of the corresponding plates.

In this work, hydro- and solvothermally prepared ZnO powders were compared with commercial ZnO and Degussa P25 TiO_2 for their efficiency in the photodegradation of RO16 azo dye in aqueous solution, using imitated sunlight illumination.

EXPERIMENTAL

Materials

All the reagents: poly(vinyl pyrrolidone), zinc acetate dihydrate, zinc nitrate hexahydrate (all Sigma Aldrich), ethylene glycol (Carlo Erba) and sodium hydroxide (*p.a.*) were of analytical grade and used without further purification. The textile dye, C.I. Reactive Orange 16, was obtained from Bezema as a gift.

Solvothermal method (ST-ZnO)

To prepare the precursor, 1.80 g of poly(vinyl pyrrolidone) (PVP) was dissolved in 75 mL of ethylene glycol (EG) and then 3.60 g of solid $Zn(CH_3COO)_2 \cdot 2H_2O$ was slowly added into the solution. The resulting mixture was stirred for several minutes, followed by the addition of 1.80 g of solid NaOH. An aliquot of 65 mL of the mixture was treated solvothermally using a Teflon®-lined stainless steel autoclave (V = 75 mL) at 120 °C for 18 h under autogenous pressure. After spontaneous cooling to room temperature, the white precipitate at the bottom of the autoclave was washed with distilled water and alcohol, and dried at 100 °C for 3 h. One part of the product was additionally heated at 300 °C for 2 h in order to investigate the influence of annealing (sample ST-ZnO-a). The mass loss during annealing was 1.9 mas. %.

Hydrothermal method (HT-ZnO)

To prepare the precursor, 50 mL of $Zn(NO_3)_2 \cdot 6H_2O$ (0.5 mol dm^{-3}) was added dropwise into 50 mL of NaOH solution (0.5 mol dm^{-3}) during 30 min under intensive stirring. The precursor mixture was further treated in the same way as described above. The mass loss during annealing was 2.7 mas. %. The annealed product was labeled as HT-ZnO-a.

Characterization techniques

X-Ray diffraction (XRD) patterns were collected over the range $20° < 2\theta < 90°$ on an Ital Structures APD2000 X-ray diffractometer using Cu*Kα* radiation (λ = 1.5418 Å). Thermogravimetric analysis (TG) was realized using an SDT Q600 instrument (TA Instruments) up to 700 °C under a dynamic air atmosphere (heating rate: 20 °C min^{-1}, flow rate: 100 mL min^{-1}). The presence of impurities was checked by Fourier transform infrared (FTIR) spectroscopy on a Bomem MB-100, Hartmann Braun FTIR spectrophotometer (range: 4000–400 cm^{-1}) using the KBr pellet technique. The size and morphology of the prepared particles were characterized using field emission scanning electron microscopy (FESEM, Tescan Mira X3).

Irradiation experiments

Photodegradation was performed using an open double-wall flask (volume 100 mL) in a dark chamber equipped with an Osram Ultra-Vitalux 300 W lamp, which produces radiation similar to the radiation of natural sunlight. The lamp was placed 50 cm away from the surface of the dye solution. Constant mixing of the solution was insured using a magnetic stirrer, while constant temperature was maintained by circulating the water through the wall of the reactor. The photodegradation of RO16 dye was studied by mixing 25 mL of an aqueous solution containing dye (50 mg dm^{-3}) and the prepared ZnO samples (50 mg) as a catalyst. The solution was then stirred to keep the suspension homogenous and left in the dark for 90 min to achieve adsorption equilibrium. Subsequently, the lamp was switched on and after 30 and 60 min of irradiation, the solution (3 mL) was sampled. The residual concentration of dye was determined using a UV–Vis spectrophotometer (Shimadzu 1700) after centrifugation of the solution. The absorption spectra and rate of photodegradation were observed in terms of

the absorbance change at the peak maximum of the dye (λ_{max} = 492.5 nm). The commercial ZnO (Orka) and Degussa P25 TiO$_2$ powders were treated in the same way for comparison.

RESULTS AND DISCUSSION

X-Ray powder diffraction, TG and FTIR analysis

The XRD patterns of all prepared samples (Fig. 1) are readily indexed to the hexagonal ZnO phase (wurtzite type structure, JCPDS card 80-0075, *a* = 3.2539 Å, *c* = 5.2098 Å). No impurities could be detected, meaning that single-phase ZnO powders were obtained using both synthetic routes. The average crystallite sizes of ZnO powders were calculated using the Scherrer formula.[13] The solvo-thermally prepared samples had a much smaller crystallite size (Table I) compared to the hydrothermally prepared ones and the commercial ZnO. This could be attributed to the already recognized role of PVP in controlling the size and shape of ZnO grains.[14] The slight increase in the unit cell parameters and crystallite sizes after annealing at 300 °C were observed in both cases. Very likely, these small changes in lattice parameters could be related to the changes in the particle sizes.[15]
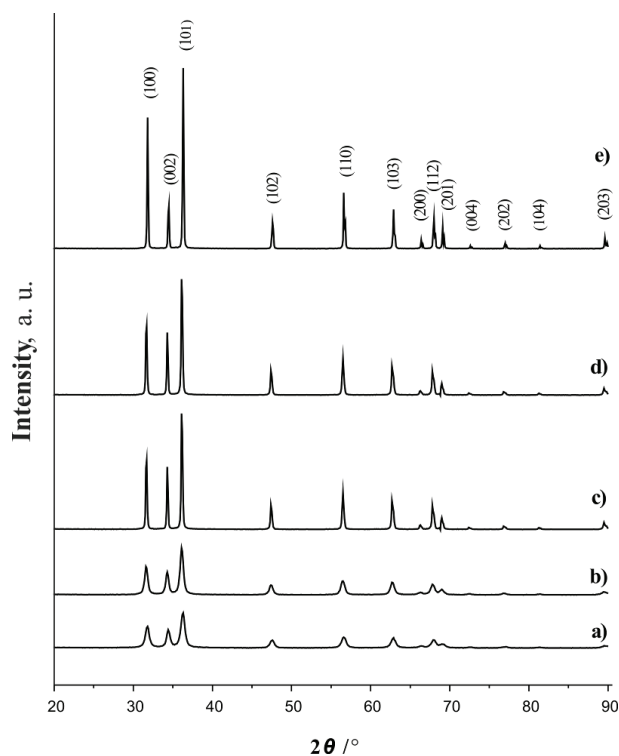

Fig. 1. XRD patterns of: a) ST-ZnO, b) ST-ZnO-a, c) HT-ZnO, d) HT-ZnO-a and e) commercial ZnO.

TABLE I. Structural and microstructural properties of the prepared ZnO materials; $<D>$ calculated by the Scherrer formula using 13 well-defined ZnO diffraction maxima

Sample	Unit cell parameters and volume a, c / Å, V / Å^3	The average crystallite size, $<D>$ / nm
ST-ZnO	$a = 3.2550(1)$, $c = 5.2107(2)$, $V = 47.812(3)$	16.7(1)
ST-ZnO-a	$a = 3.2571(1)$, $c = 5.2215(2)$, $V = 47.971(3)$	21.1(3)
HT-ZnO	$a = 3.2452(1)$, $c = 5.1980(4)$, $V = 47.407(3)$	71.7(5)
HT-ZnO-a	$a = 3.2556(1)$, $c = 5.2143(2)$, $V = 47.861(3)$	75.0(5)
Commercial ZnO	$a = 3.2491(1)$, $c = 5.2028(2)$, $V = 47.570(3)$	94.6(1)

The TG curves are shown in Fig. 2. The annealed HT-ZnO-a sample (Fig. 2, curve e) and commercial ZnO (Fig. 2, curve d) showed almost negligible mass loss (less than 1.0 mas. %), probably due to their slightly hygroscopic nature. The ST-ZnO-a sample (Fig. 2, curve c) showed a little greater mass loss (about 2 mas. %) that could be ascribed to the better H_2O adsorption due to nanosize effects. As expected for the non-annealed samples (Fig. 2, curves a and b), a higher total mass loss (about 3.0 mas. %) was obtained. In the case of the HT-ZnO sample (Fig. 2, curve a), an abrupt loss at about 250 °C very likely corresponds to the decomposition of $Zn(NO_3)_2$.[16]
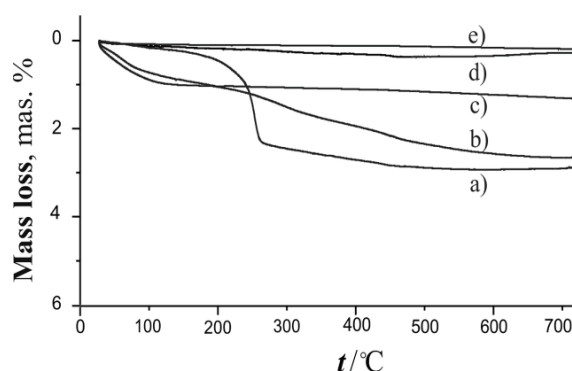

Fig. 2. TG curves of: a) HT-ZnO, b) ST-ZnO, c) ST-ZnO-a, d) commercial ZnO and e) HT-ZnO-a.

The ST-ZnO (Fig 2, curve b) sample is similar to HT-ZnO, but the process has no clearly distinguished steps or thermal effects. Considering this result, the mass loss could be attributed to the simultaneous decomposition of traces of acetate ions and PVP.[17,18]

Considering the FTIR spectra (Fig. 3), the intensive band at around 480 cm^{-1} is characteristic for Zn–O stretching vibrations.[19] The bands at 2850 and 2920 cm^{-1} correspond to the $\nu(CH_2)$ vibrations. The bands at around 1640 and 1400 cm^{-1} could be attributed to the asymmetrical and symmetrical stretching of the COO groups, respectively. The appearance of these bands supports the pre-

sence of acetate groups, although residual PVP could not be totally excluded. However, these bands also existed in the spectrum of the commercial ZnO and agree with the corresponding literature data,[20] *i.e.*, the commercial and the herein described ZnO have identical FTIR spectra. The broad bands centered at about 3440 cm^{-1} could be attributed to the ν(OH) vibrations that arise from the slightly hygroscopic nature of ZnO and the consequential surface adsorption of ambient water.[20] According to the mass loss during annealing of the ST-ZnO sample, the percentage of hygroscopic H_2O was lower than 2 mas. %.
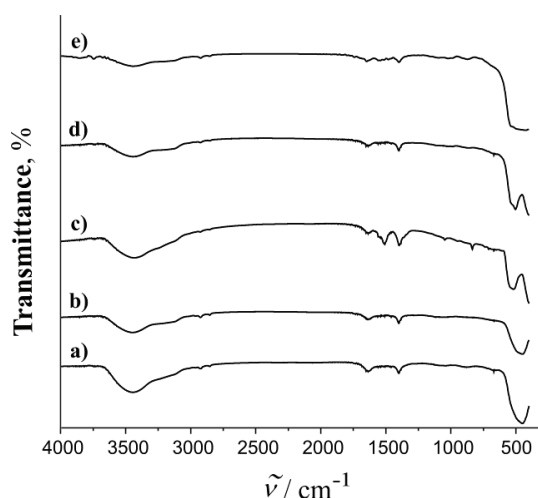
Fig. 3. FTIR spectra of: a) ST-ZnO, b) ST-ZnO-a, c) HT-ZnO, d) HT-ZnO-a and e) commercial ZnO.

The bands due to the N–O stretch at 1515–1560 cm^{-1} in the spectrum of the HT-ZnO sample disappeared after annealing, meaning that the residual nitrate ions were easily decomposed at 300 °C, which confirmed the TG results. Regarding the results of XRD analysis and the mass loss during annealing, the content of impurities in the as-prepared HT-ZnO sample should be less than 3 mas. %.

Morphology of the nanostructures

The morphologies of the prepared ZnO powders were very different. The commercial ZnO (Fig. 4, a) consisted of hexagonal prisms of different sizes, with diameters between 50 and 500 nm and lengths from 100 to 700 nm.

The HT-ZnO and HT-ZnO-a particles shown in Fig. 4, b and c, were very similar in size and morphology. Both samples consisted of hexagonal shaped rods with diameters of up to 800 nm and the lengths up to several micrometers, but HT-ZnO-a had more uniformly distributed dimensions. Identical, sometimes hollowed rods were obtained previously when water was used as the medium.[4] In addition, there was a small amount of web-like nanofibers in HT-ZnO, and a small quantity of nanograins in the HT-ZnO-a sample. Thus, in both cases, a bimodal grain size distribution with a great predominance of rods was observed.
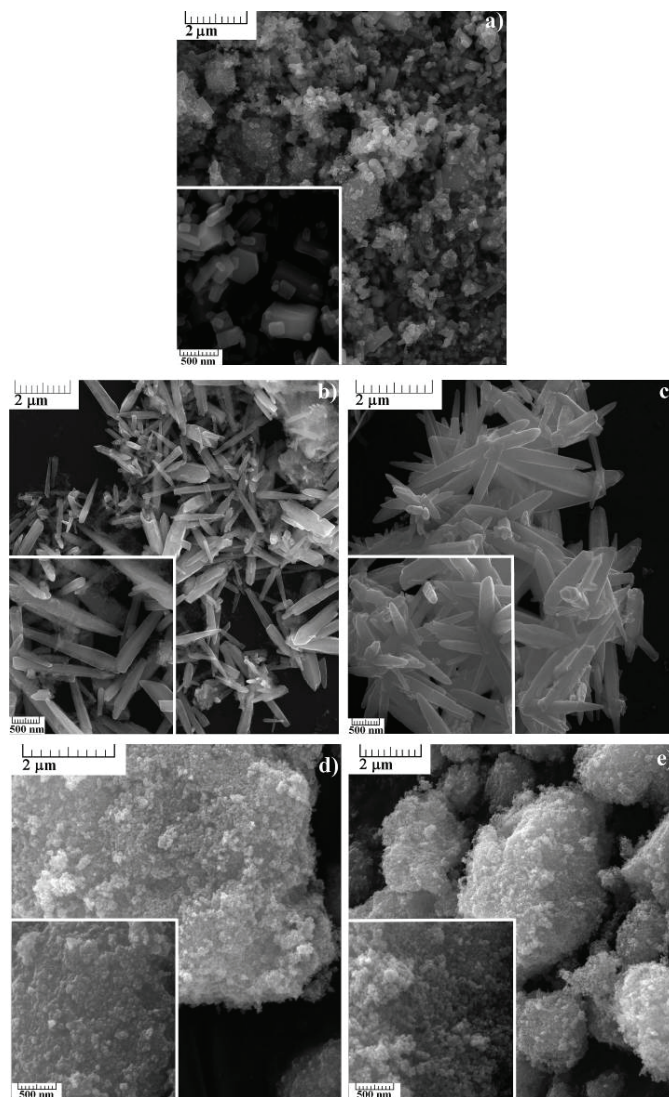
Fig. 4. FESEM images of: a) commercial ZnO, b) HT-ZnO rods, c) HT-ZnO-a rods,
d) ST-ZnO nanopowder and e) ST-ZnO-a nanopowder.

The ST-ZnO and ST-ZnO-a particles (Fig. 4, d and e) were also related. Precisely, they consisted of small (<50 nm), rounded nanograins, creating very loosely packed aggregates. PVP played an important role in controlling the size and shape of the ZnO particles during the synthesis. Here, PVP together with EG, limited the growth of the ZnO particles probably along all crystal planes, causing the uniformity in size and approximately spherical shape of the particles.[21]

Photodegradation of RO16 dye

As shown in Fig. 5, all the prepared ZnO materials had a higher efficiency in the photodegradation of RO16 dye than the commercial ZnO. The results also indicated that non-annealed samples of ZnO had a higher photocatalytic efficiency than Degussa P25 TiO$_2$, which is the standard material in the field of photocatalytic reactions. After 30 min, the effectivenesses of the solvothermally prepared samples and commercial ZnO were approximately the same. However, the efficiency of commercial ZnO markedly decreased after 60 min, whereas the as-prepared samples were more efficient, resulting in almost complete degradation of RO16 dye. In total, the ST-ZnO nanoparticles were slightly more efficient than the HT-ZnO rods, probably due to the smaller size and higher active surface area. In addition, the smaller sizes of the crystallites in the ST-ZnO samples, inherently meaning a higher number of defects, should be taken into account. Nevertheless, none of these factors had a significant influence on the photodegradation process, as shown by very similar efficiencies of all samples.
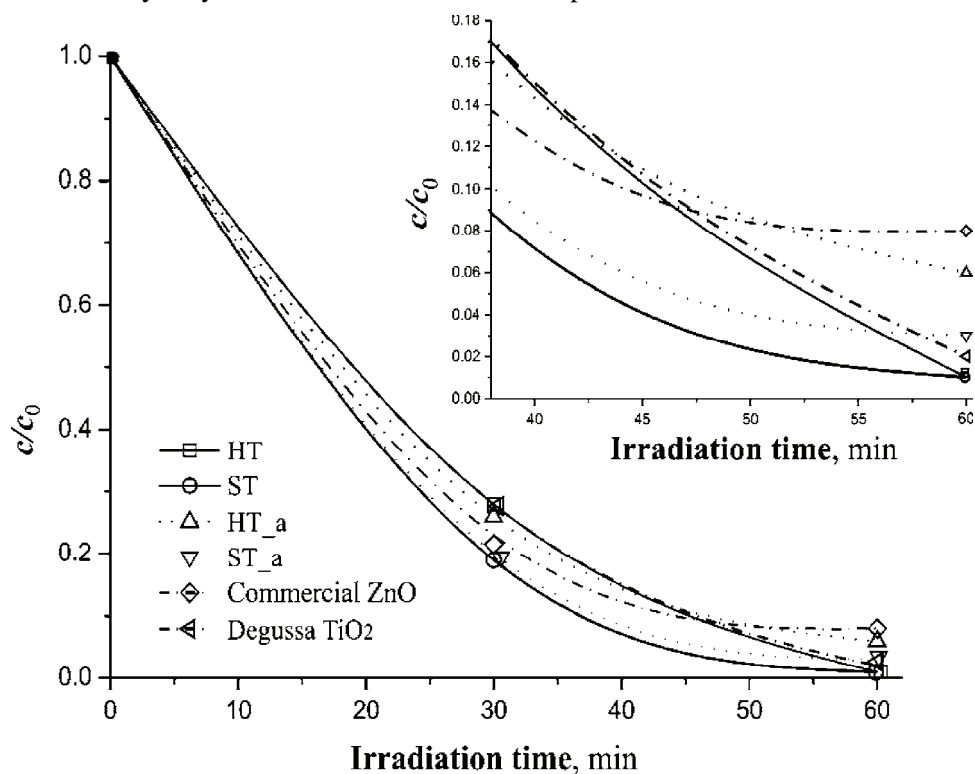

Fig. 5. The rate of photodegradation of RO16. The inset shows the activity between 35 and 60 min.

The order of decreasing activity was ST-ZnO > HT-ZnO > Degussa P25 TiO$_2$ > ST-ZnO-a > HT-ZnO-a > commercial ZnO. A negligible decrease of photocatalytic activity was observed after annealing; this could be assigned to the increasing of crystallite sizes and changes in porosity.

A comparison with three already mentioned papers[10–12] was difficult, since Dhodapkar *et al.*[10] reported the results of RO16 degradation using natural sunlight, while in the other two studies,[11,12] a UV lamp was used and the ZnO catalyst was in the form of a stationary layer. Moreover, different dye concentrations and doses of the photocatalysts were applied. Generally, it is challenging to compare the efficiency of photocatalysts because the published studies were, as a rule, performed under different conditions, which had to be taken into account.[22,23] For these reasons, in this paper, the efficiency of the photocatalysts prepared under the same conditions was compared in order to select a better procedure for future research.

CONCLUSIONS

Two ZnO powders with diverse morphologies were prepared by the hydrothermal and solvothermal methods. The phase purity of the samples was confirmed by XRD analysis, although a small amount of residual NO$_3^-$ groups was detected by FTIR analysis in the as-prepared HT-ZnO sample. These impurities were easily removed by annealing at 300 °C for 2 h. In summary: a) all prepared ZnO samples had a high efficiency for the photodegradation of RO16 textile dye; b) both non-annealed samples were more active than commercial ZnO, especially when the concentration of the dye was low; c) both non-annealed samples had a slightly higher efficiency than the commercial Degussa P25 TiO$_2$; d) the solvothermally prepared, non-annealed ZnO particles were found to be the most efficient photocatalysts, exhibiting slightly higher activity than the hydrothermally as-prepared rods; e) application of the surfactant PVP was directly related to small crystallite and particle sizes, and for this reason, it is recommended the use of this polymer in future studies for this application; f) the photocatalytic activity of the ZnO materials depended much neither on the crystallite and particle size nor on the morphology; g) the presence of impurities in the as-prepared samples and their further annealing had only a minor influence on their photocatalytic activity. Therefore, the photocatalytic degradation of textile dyes and textile effluent assisted with ZnO materials might be an economic, environmentally friendly and efficient method for water treatment.

И З В О Д

ХИДРО- И СОЛВОТЕРМАЛНО ПРИПРЕМЉЕН ZnO И ЊЕГОВ КАТАЛИТИЧКИ УТИЦАЈ НА ФОТОДЕГРАДАЦИЈУ БОЈЕ *REACTIVE ORANGE* 16

БОЈАНА СИМОВИЋ[1], АЛЕКСАНДАР ГОЛУБОВИЋ[2], ИВАНА ВЕЉКОВИЋ[3], ДЕЈАН ПОЛЕТИ[4], ЈЕЛЕНА ЗДРАВКОВИЋ[5], ДУШАН МИЈИН[4] и АНЂЕЛИКА БЈЕЛАЈАЦ[5]

[1]*Институт за мултидисциплинарна истраживања, Универзитет у Београду, Кнеза Вишеслава, 11030 Београд,* [2]*Институт за физику, Универзитет у Београду, Прегревица 118, 11080 Београд-Земун,* [3]*The Netherlands Organization for Applied Scientific Research – TNO, De Rondom 1, Eindhoven, The Netherlands,* [4]*Катедра за општу и неорганску хемију, Технолошко–металуршки факултет, Универзитет у Београду, Карнегијева 4, 11120 Београд, и* [5]*Иновациони центар Технолошко–металуршког факултета, Универзитет у Београду, Карнегијева 4, 11120 Београд*

У овом раду, прахови цинк-оксида синтетисани су на два различита начина: хидро- и солвотермалном синтезом полазећи, истим редом, од $Zn(NO_3)_2$ и $Zn(CH_3COO)_2$. Оба тако припремљена узорка су потом жарена на благим условима (300 °C) да би се избегао раст зрна и да би се уклонили трагови нечистоћа. Испитан је утицај начина синтезе на структурна, микроструктурна, термичка и фотокаталитичка својства добијених прахова ZnO. Рендгенском дифракцијом праха потврђено је присуство само једне фазе, хексагоналног ZnO у сва четири узорка. Морфологије добијених прахова ZnO биле су различите и варирале су од нанозрна приближно сферног облика до микроштапића. Сви припремљени узорци показују већу фотокаталитичку ефикасност него фабрички ZnO у деградацији комерцијалне текстилне азо боје *Reactive Orange* 16. Такође, нежарени узорци имају нешто боља фотокаталитичка својства него фабрички TiO_2 прах Degussa P25.

(Примљено 20. маја, ревидирано 14. јула, прихваћено 17. јула 2014)

REFERENCES

1. C. Wang, E. Shen, E. Wang, L. Gao, Z. Kang, C. Tian, Y. Lan, C. Zhang, *Mater. Lett.* **59** (2005) 2867
2. C. Wu, X. Qiao, J. Chen, H. Wang, F. Tan, S. Li, *Mater. Lett.* **60** (2006) 1828
3. R. Andreozzi, V. Caprioa, A. Insola, R. Marotta, *Catal. Today* **53** (1999) 51
4. L. Xu, Y. L. Hu, C. Pelligra, C. H. Chen, L. Jin, H. Huang, S. Sithambaram, M. Aindow, R. Joesten, S. L. Suib, *Chem. Mater.* **21** (2009) 2875
5. S. Sakthivel, B. Neppolian, M. V. Shankar, B. Arabindoo, M. Palanichamy, V. Murugesan, *Sol. Energ. Mat. Sol., C* **77** (2003) 65
6. A. Akoyl, H. C. Yatmaz, M. Bayramoglu, *Appl. Catal., B* **54** (2004) 19
7. A. Pandurangam, P. Kamala, S. Uma, M. Palanichamy, V. Murugesan, *Indian J. Chem. Technol.* **8** (2001) 496
8. N. Daneshvar, D. Salari, A. R. Khataee, *J. Photochem. Photobiol., A* **157** (2003) 111
9. S. K. Asl, S. K. Sadrnezhaad, M. K. Rad, D. Uner, *Turk. J. Chem.* **36** (2012) 121
10. R. S. Dhodapkar, V. Chaturvedi, N. R. Neti, S. N. Kaul, *Ann. Chim.* **93** (2003) 739
11. E. Yassıtepe, H. C. Yatmaz, C. Ozturk, K. Ozturk, C. Duran, *J. Photochem. Photobiol., A* **198** (2008) 1
12. L. S. Roselin, R. Selvin, *Sci. Adv. Mater.* **3** (2011) 251
13. H. P. Klug, L. E. Alexander, *X-Ray Diffraction Procedures*, 2nd Ed., Wiley, New York, 1974, p. 687
14. T. Thilagavathi, *J. Nanomater.* **2013** (2013) 7
15. M. Hosokawa, K. Nogi, M. Naito, T. Yokoyama, *Nanoparticle Technology Handbook*, Elsevier, Amsterdam, 2007, p. 644

16. M. Maneva, N. Petrov, *J. Therm. Anal.* **35** (1989) 2297
17. D. L. Golić, G. Branković, M. P. Nešić, K. Vojisavljević, A. Rečnik, N. Daneu, S. Bernik, M. Šćepanović, D. Poleti, Z. Branković, *Nanotechnology* **22** (2011) 395603
18. C. Song, X. Dong, *Adv. Chem. Eng. Sci.* **2** (2012) 108
19. R. Y. Hong, J. H. Li, L. L. Chen, D. Q. Liu, H. Z. Li, Y. Zheng, J. Ding, *Powder Technol.* **189** (2009) 426
20. G. Xiong, U. Pal, J. G. Serrano, K. B. Ucer, R. T. Williams, *Phys. Stat. Sol., C* **3** (2006) 3577
21. D. Yiamsawas, K. Boonpavanitchakul, W. Kangwansupamonkon, *J. Micros. Soc. Thailand* **23** (2009) 75
22. S. M. Lam, J. C. Sin, A. Z. Abdullah, A. R. Mohamed, *Desalin. Water Treat.* **41** (2012) 131
23. S. Ahmed, M. G. Rasul, W. N. Martens, R. Brown, M. A. Hashib, *Water Air Soil Pollut.* **215** (2011) 3.